Extensional wave attenuation and velocities in partially saturated unconsolidated sand at sonic frequencies

Zhuping Liu[1], Kurt T. Nihei, Seiji Nakagawa, Liviu Tomutsa and Larry R. Myer

Earth Sciences Division, Lawrence Berkeley National Laboratory, Berkeley, California

Abstract. Extensional wave attenuation and velocity measurements on a high permeability Monterey sand were performed over a range of gas saturations for imbibition and degassing conditions. These measurements were conducted using extensional wave pulse propagation and resonance over a 1 – 9 kHz frequency range for a hydrostatic confining pressure of 8.3 MPa. Analysis of the extensional wave data and the corresponding X-ray CT images of the gas saturation show strong attenuation resulting from the presence of the gas (Q_E dropped from 300 for the dry sand to 30 for the partially-saturated sand), with larger attenuation resulting from heterogeneous gas distributions. The extensional wave velocities are in agreement with Gassmann theory for the test with near-homogeneous gas saturation and with a patchy saturation model for the test with heterogeneous gas saturation. These results show that partially saturated sands under moderate confining pressure can produce strong intrinsic attenuation for extensional waves.

[1] Also at University of California, Berkeley, California; Now at Shell Exploration and Production Company, New Orleans, Louisiana.

1. Introduction

The acoustic properties of poorly consolidated sands is a topic of importance in a number of fields, including geotechnical investigation of soil properties for stability (Stoll, 1989; Ishihara, 1996), environmental monitoring of contaminants in the shallow subsurface (Geller and Myer, 1995; Seifert et al., 1998), and geophysical characterization of sand reservoirs and aquifers for petroleum production (Gardner et al., 1964; Domenico, 1976, 1977; Spencer et al., 1994; Prasad, 2002) and CO_2 sequestration (Eiken et al., 2000). While many studies have documented the velocities of dry and saturated sands over a range of confining pressures, fewer studies have examined the velocities and attenuation of poorly consolidated sands under conditions of partial saturation, elevated confining pressures, and at sonic frequencies (1-20 kHz).

Systematic studies of the velocities and attenuation of poorly consolidated sands under these conditions can provide valuable data to test current theories for the effective moduli and attenuation for granular, porous materials (e.g., see Mavko et al., 1998). The overall objective of our research program on sands is to investigate the role of partial gas saturation on the attenuation and velocity of acoustic waves in the seismic to sonic frequency range (1 Hz to 20 kHz) over a range of confining pressures. As a first step towards this goal, we have developed a sonic frequency apparatus that utilizes resonance and pulse propagation to measure the velocities and attenuation of poorly consolidated sands under hydrostatic confinement. The confining vessel is fabricated of aluminum, allowing the gas and fluid phases to be imaged with an X-ray CT scanner. In this paper, we report our recent efforts to measure the extensional wave velocities and attenuation of Monterey sand with homogeneous and heterogeneous distributions of gas.

2. Extensional Wave Resonance and Pulse Propagation Tests

2.1 Sample Properties

The sand used in the extensional wave tests is coarse grain Monterey sand (Lonestar 2/12). The sand was first washed to remove the fines, and sieved to achieve an average grain diameter of 1.21 mm. The sand was packed by pluviation from a constant height of fall and rate of flow. The dry density of the sand packing is 1.73 g/cc. The porosity measured via the gas expansion method is 34.6%. Constant flow rate measurements on the sand packing revealed that the sample permeability is ≥ 30 D.

2.2 Description of the Experiment

The experimental apparatus for the sonic frequency extensional wave velocity and attenuation measurements incorporates a thin polycarbonate tube (0.577 mm wall thickness) to house the sand (Figure 1). The sample length is 0.814 m, and the diameter is 43 mm. Nitrogen gas rather than a fluid is used as the confining medium to minimize the acoustic coupling of the sample to the confining vessel. The ends of the sample are mass-loaded with stainless steel transducers that house the piezoelectric source and receiver and contain fluid feedthroughs for pore fluid injection and withdrawal. The added mass of the transducers lowers the resonance frequency of the sample and also reduces the acoustic radiation between the sample and the confining vessel by altering the boundary conditions at the ends of the bar from a zero-stress boundary to something approaching a zero-displacement boundary. The confining vessel is fabricated of aluminum to allow X-ray CT scanning of the sand pack during the test.

Acoustic measurements are performed by exciting one end of the sample with an extensional mode piezoelectric PZT crystal and recording the resulting particle acceleration on the opposite end of the sample with a miniature, three-component accelerometer. Resonance and pulse propagation measurements are performed by driving the piezoelectric crystal with a chirp signal for the former, and a Ricker wavelet, for the latter.

2.3 Data Processing

2.3.1 Pulse Propagation

Waveforms obtained from the extensional wave pulse propagation test for dry Monterey sand with a hydrostatic confining pressure of 8.3 MPa show clear first arrivals followed by a series of multiple reflections (top waveform, Figure 2). Increasing water saturation results in a clear reduction in the amplitudes, and an increase in the travel times of all the arrivals, except at the highest saturations where the trend reverses. Extensional wave phase velocities and attenuation estimates are obtained from these waveforms by forming spectral ratios between the recorded particle acceleration of any two arrivals.

Because of the one-dimensional nature of extensional wave propagation in a bar, geometrical spreading is negligible. Additionally, if the wavelength is much larger than the bar diameter, velocity dispersion is small and can be neglected. Under these conditions, the phase velocity c and quality factor Q (assuming $Q > 1$) can be computed from the frequency spectra of the measured particle acceleration data a_1 and a_2 using $c = \omega \triangle L / \triangle \varphi$ and $Q = \omega \triangle L / [2c \ln(a_1/a_2)]$, where ω is the angular frequency, $\triangle L$ is the difference in the travel distances taken by pulses *1*

and *2*, and $\triangle\varphi$ is the phase difference between pulses *1* and *2*. Once the velocities are obtained, they must be corrected for the stiffening effect of the jacket. For extensional modes in the long wavelength limit (relative to the diameter), the phase velocity of the fundamental extensional mode is given by (Lai et al., 1971)

$$c_E = \left[\frac{E_2[(R^2-1)+(E_1/E_2)]}{\rho_2[(R^2-1)+(\rho_1/\rho_2)]} \right]^{1/2}, \tag{1}$$

where E is the Young's modulus, ρ is the density, $R = r_2/r_1$ is the ratio of the outer and inner radii of the jacketed sample, and the subscripts *1* and *2* refer to the sample and jacket, respectively.

2.3.2 Resonance

Spectra obtained from the resonance tests for conditions corresponding to Figure 2, are displayed in Figure 3. Increasing water saturation results in a clear broadening and reduction in the amplitudes of the resonance peaks, and a downward shift in the resonance frequencies, except at the higher saturations where the trend reverses. Extensional wave attenuation estimates are obtained for the first several extensional resonance modes via the half-power method, $Q = \omega_n / \triangle\omega$, where $\triangle\omega_n$ is the spectral width of the power spectrum of the n^{th} mode at half spectral power. Extensional wave phase velocities cannot be computed directly from the resonance frequencies using the standard relation for a bar with zero-stress ends because the massive transducers on the ends of the bar lower the resonance frequencies. A finite element method based modal code (Nakagawa, 1998) capable of modeling the jacket contribution and the

added mass of the two transducers, is used in an iterative matching algorithm to determine the Young's modulus of the sand pack.

3. Results

3.1 Fluid and Gas Distributions

The results of three tests with different distributions of gas are reported in this section. The three tests started with the same procedure: a room dry sand sample was subjected to 8.3 MPa hydrostatic confining pressure, rotated to a vertical position, and flushed with several pore volumes of CO_2 gas from the bottom of the sample.

Near *homogeneous* gas distributions (Figure 4a) were achieved by first injecting several pore volumes of de-aired distilled water into the bottom of the sample while in the vertical position, followed by injection of carbonated water into the sample at a pressure of approximately 1 MPa. Next, the sample was rotated to the horizontal position and placed in the X-ray CT scanner for pore scale imaging of the fluid and gas phases. Acoustic measurements were performed between scans as the pore pressure was dropped below the CO_2 degassing pressure (~0.3 MPa).

Two types of heterogeneous (i.e., patchy) gas distributions were achieved by the following approaches. Data obtained while the initially dry sample was kept in a vertical configuration and flooded with water from the bottom of the sample represents the *patchy-vertical* case. For this configuration, it was not possible to CT scan the sample. However, because of the loose packing structure of the coarse grain sand pack and the low flow rate, it is expected that the water injected from the bottom of the sample moved upward as a stable front.

The second style of patchy gas saturation was obtained by injecting water into the initially dry sand pack while it was oriented in a horizontal position. This configuration produced a gas cap at the top of the sample and is referred to as the *patchy-horizontal* case (Figure 4b).

3.2 Extensional Wave Attenuation and Velocities

Extensional wave velocities and attenuation were calculated from the pulse transmission and resonance data using the procedures described in Section 2.3. The attenuation and velocities obtained from these two methods showed good agreement, and we report here only the velocities obtained from the pulse propagation data and the attenuation computed from the resonance data.

The extensional wave velocities and attenuation at 3 kHz for the three different distributions of gas are displayed in Figure 5. The velocities show a gradual decrease with increasing water saturation, followed by a sharp increase at near full saturation. The attenuation show a monotonic increase with increasing water saturation (Q decreases from ~300 in the dry sand packing to ~30 at near full saturation), followed by an abrupt drop at full saturation. The velocities and attenuation for the homogeneous case are lower than those obtained for the two patchy cases.

4. Discussion

The extensional wave velocities for the homogeneous case are well described by Gassmann's relation for a poroelastic material (e.g., Berryman et al., 2000).

$$K = K_{dr} + \frac{\alpha^2}{(\alpha - \phi)/K_m + \phi/K_f} \quad and \ \mu = \mu_{dr}, \tag{2}$$

where K_m is the bulk modulus of the grain material, K_{dr} and μ_{dr} are the bulk and shear moduli of the drained porous frame, $\alpha = 1 - K_{dr}/K_m$ is the Biot-Willis parameter, ϕ is the porosity, and K and μ are the effective bulk and shear moduli of the undrained, partially-saturated porous medium. For homogeneous mixing of liquid and gas within the pore space, the bulk modulus of the fluid-gas mixture K_f can be computed from an isostress (Reuss) average (e.g., Mavko et al., 1998),

$$\frac{1}{K_f} = \frac{S}{K_{fluid}} + \frac{(1-S)}{K_{gas}}, \tag{3}$$

where S is the fluid saturation. The prediction of Gassmann's relation (assuming μ=1.13 GPa), displayed in Figure 6, shows good agreement with the experimental velocities for the homogeneous saturation case. This result suggests the pore fluid pressures have equilibriated throughout the pore space as the 3 kHz pulse propagates through the sand pack.

Analysis of the velocities for the patchy-vertical case yields favorable agreement with a patchy saturation model that consists of forming the harmonic average of the Lamé constant λ of the dry and fully water-saturated patches (i.e., Hill's relation for two materials with identical shear moduli; Mavko et al., 1998), each with properties described by Gassmann's relation (2),

$$K = \left(\frac{S}{K_{G-wat} + \frac{4}{3}\mu} + \frac{(1-S)}{K_{G-dry} + \frac{4}{3}\mu} \right)^{-1} - \frac{4}{3}\mu, \tag{4}$$

where K_{G-wat} and K_{G-dry} are the bulk moduli of the completely water-saturated and completely dry sand computed using Gassmann's relation (2). Again assuming μ =1.13 GPa, good agreement is obtained with Hill's equation (4) and the velocity measurements for the patchy-vertical configuration (Fig. 6). The higher velocities are indicative of a stiffer system that results from unequilibrated pore fluid pressures within water-saturated portion of the sand pack.

The patchy-horizontal system yields velocities that fall between the homogeneous and patch-vertical data. This is somewhat expected since the pore fluid pressure can equilibrate along the lower half of the sample where a continuous layer of water is present.

While the velocities for the homogeneous and patchy-vertical gas saturations can be explained with existing theories, the source of the strong extensional wave attenuation needs to be explored further. A possible mechanism for the strong observed attenuation is the White mechanism (White, 1975; Dutta and Ode, 1979a,b; Dutta and Seriff, 1979) resulting from wave conversions from a compressional wave (or extensional wave) into a diffusive slow wave at the water-gas patch boundaries. Refinements and applications of this mechanism for compressional wave attenuation and velocity dispersion have been the subject of several recent papers (Johnson, 2001; Quiroga-Goode, 2001; Tserkovnyak and Johnson, 2002).

Finally, it is worth noting that the observed velocities and attenuation in the poorly consolidated sand used in this study is of a similar nature to that observed in a number of laboratory studies on consolidated rocks, including sandstones (Yin et al., 1992) and limestones (Cadoret et al., 1998). These studies show that small amounts of gas in the form of isolated gas patches can produce strong attenuation of seismic frequency (1-100 Hz) and sonic frequency (5-

20 kHz) waves. The results of this study (Figure 5) suggest that similar effects can occur in highly permeable sands.

In future work, we will examine the possibility of poroelastic losses resulting from gas patches using numerical simulations with gas distributions obtained from the CT scans. Additionally, this work on extensional waves will be supplemented with new source and receiver transducers capable of measuring both extensional and torsional waves, allowing us to measure two elastic moduli and torsional and extensional attenuation during a single test. In these tests, we hope to measure the viscoelastic properties of unconsolidated sands over a broad range of confining pressures.

Acknowledgments. This research was supported by the Assistant Secretary of Fossil Energy, National Petroleum Office, and by the Director, Office of Energy Research, Office of Basic Energy Sciences, both under U.S. Department of Energy Contract No. DE-AC03-76SF00098.

References

Berryman, J. G., P. A. Berge, B. P. Bonner, Transformation of seismic velocity data to extract porosity and saturation values for rocks, *J. Acoust. Soc. Am.,* 107, 3018-3027, 2000.

Cadoret, T., G. Mavko, B. Zinszner, Fluid distribution effect on sonic attenuation in partially saturated limestones, *Geophys*., 63, 154-160, 1998.

Domenico, S. N., Effect of brine-gas mixture on velocity in an unconsolidated sand reservoir, *Geophys.*, 41, 882-894, 1976.

Domenico, S. N., Elastic properties of unconsolidated porous sand reservoirs, *Geophys.*, 42, 1339-1368, 1977.

Dutta, N. C., H. Odé, Attenuation and dispersion of compressional waves in fluid-filled rocks with partial gas saturation (White Model)-Part I: Biot theory, *Geophys.*, 44, 1777-1788, 1979a.

Dutta, N. C., H. Odé, Attenuation and dispersion of compressional waves in fluid-filled rocks with partial gas saturation (White Model)-Part II: Results, *Geophys.*, 44, 1789-1805, 1979b.

Dutta, N. C., A. J. Seriff, On White's model of attenuation in rocks with partial gas saturation, *Geophys.*, 44, 1806-1812, 1979.

Eiken, O., I. Brevik, E. Lindeberg, K. Fagervik, Seismic monitoring of CO_2 injected into a marine aquifer, *Expanded Abstracts*, 70th Annual Meeting of the Soc. Expl. Geophys., Calgary, 1623-1626, 2000.

Gardner, G. H. F., M. R. J. Wyllie, D. M. Droschak, Effects of pressure and fluid saturation on the attenuation of elastic waves in sands, *J. Petrol. Tech*., 189-198, 1964.

Geller, J., L. Myer, Ultrasonic imaging of organic contaminants in unconsolidated porous media, *J. Contam. Hydrol*., 19, 85-104, 1995.

Ishihara, K., *Soil Behaviour in Earthquake Geotechnics,* Oxford Univ. Press, Oxford, 1996.

Johnson, D. L., Theory of frequency dependent acoustics in patchy-saturated porous media, *J. Acoust. Soc. Am.*, 110, 682-694, 2001.

Lai, J.-L., E. H. Dowell, T. R. Tauchert, Propagation of harmonic waves in a composite elastic cylinder, *J. Acoust. Soc. Am*., 49, 220-228, 1971.

Mavko, G., T. Mukerji, J. Dvorkin, *Rock Physics Handbook*, Cambridge Univ. Press, Cambridge, 1998.

Nakagawa, S., *Acoustic Resonance Characteristics of Rock and Concrete Containing Fractures*, Ph.D. Thesis, Univ. of California at Berkeley, 1998.

Prasad, M., Acoustic measurements in unconsolidated sands at low effective pressure and overpressure detection, *Geophys.*, 67, 405-412, 2002.

Quiroga-Goode, G., Dynamics of Biot squirt-flow, *Acoust. Res. Lett. Online*, 3, 12-17, 2001.

Seifert, P., J. Geller, L. R. Johnson, Effect of P-wave scattering on velocity and attenuation in unconsolidated sand saturated with immiscible liquids, *Geophys*., 63, 161-170, 1998.

Spencer, J. W., M. E. Cates, D. D. Thompson, Frame moduli of unconsolidated sands and sandstones, *Geophys.*, 59, 1352-1361, 1994.

Stoll, R. D., *Sediment Acoustics*, Springer, Berlin, 1989.

Tserkovnyak, Y., D. L. Johnson, Can one hear the shape of a saturation patch?, Geophys. Res. Lett., 29, **12**-1-**12**-4 , 2002.

White, J. E., Computed seismic speeds and attenuation in rocks with partial gas saturation, *Geophys.*, 40, 224-232, 1975.

Yin, C.-S., M. L. Batzle, B. G. Smith, Effects of partial liquid/gas saturation on extensional wave attenuation in Berea sandstone, *Geophys. Res. Lett*., 19, 1399-1402, 1992.

Figure Captions

Figure 1. Photograph of experimental apparatus: aluminum confining vessel (background), and sand packing housed in a thin polycarbonate tube with stainless steel transducers containing acoustic source and receiver (foreground).

Figure 2. Pulse propagation data (3 kHz wavelet) for Monterey sand with 8.3 MPa hydrostatic confining pressure for a range of saturations. Clear first arrivals and six multiple reflections are observable on each trace.

Figure 3. Resonance data (0-10 kHz) for Monterey sand with 8.3 MPa hydrostatic confining pressure for a range of saturations. Clear fundamental extensional resonance peaks and higher order harmonics are evident on each spectrum.

Figure 4. Water saturations obtained from X-ray CT scanning the sand samples: (a) *homogeneous* case with uniform distribution of water and gas (20 mm slices with 0.2 mm resolution; average water saturation is 90%), and (b) *horizontal-patchy* case with gas cap along the top (10 mm slices with 0.2 mm resolution; average water saturation is 60%). The length of the image is 81 cm, and the diameter is 43 mm.

Figure 5. Extensional wave velocities and attenuation at 3 kHz for a range of water saturations and for three types of gas saturation: homogeneous, patchy-horizontal, and patchy-vertical.

Figure 6. Comparison of measured extensional wave velocities with Gassmann theory (homogeneous case) and Hill+Gassmann (patchy-vertical case).

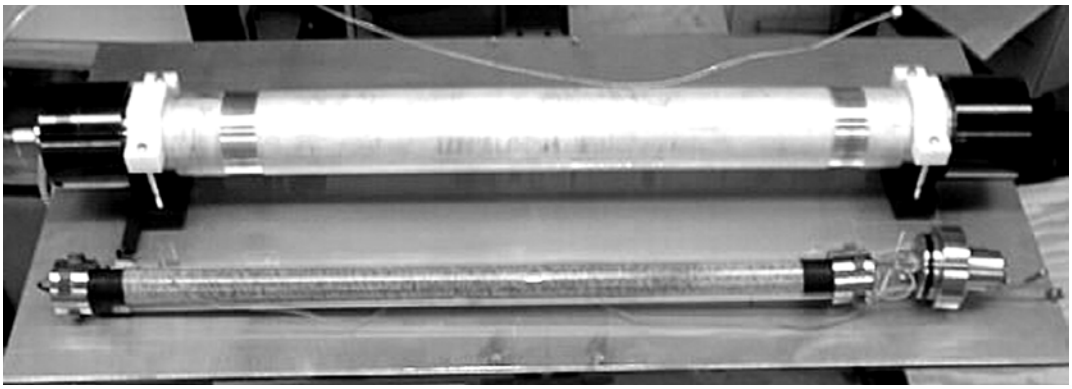

Figure 1. Photograph of experimental apparatus: aluminum confining vessel (background), and sand packing housed in a thin polycarbonate tube with stainless steel transducers containing acoustic source and receiver (foreground).

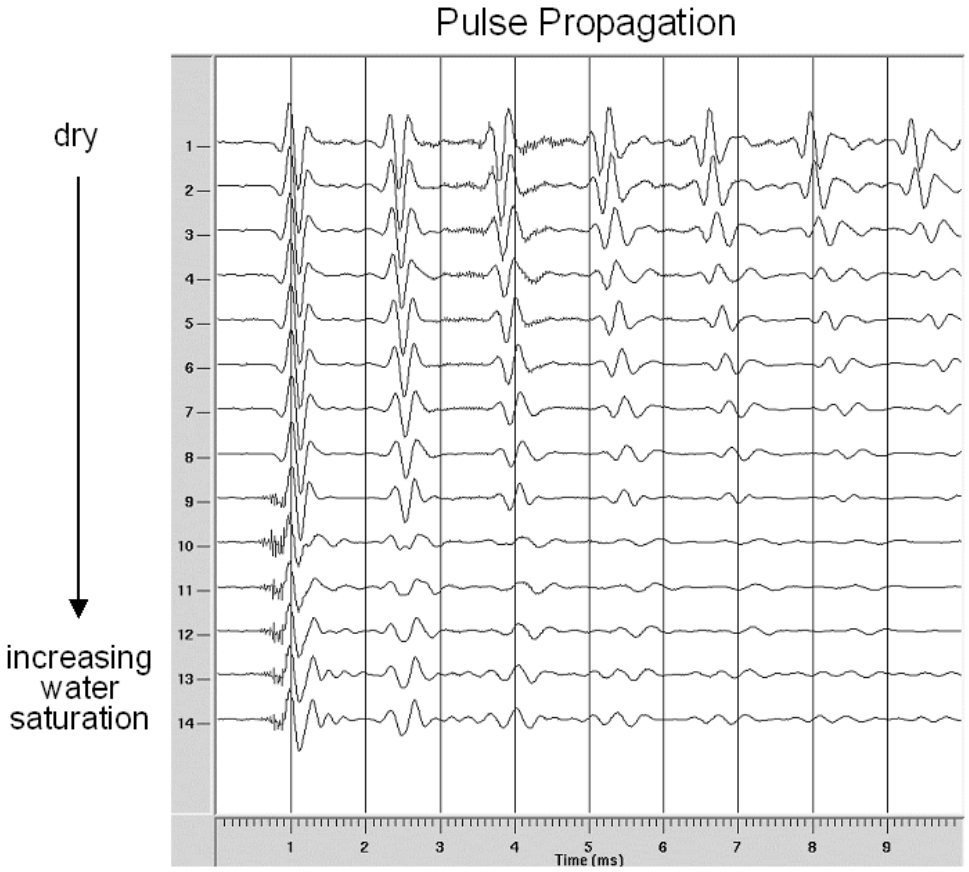

Figure 2. Pulse propagation data (3 kHz wavelet) for Monterey sand with 8.3 MPa hydrostatic confining pressure for a range of saturations. Clear first arrivals and six multiple reflections are observable on each trace.

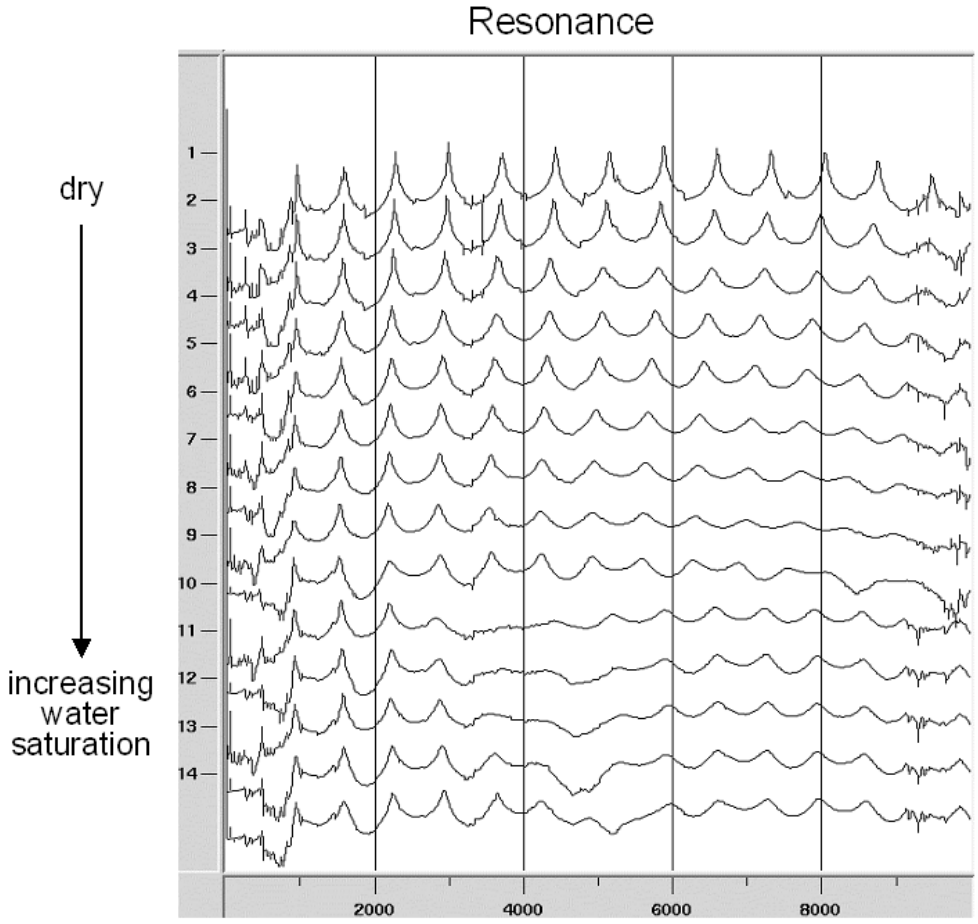

Figure 3. Resonance data (0-10 kHz) for Monterey sand with 8.3 MPa hydrostatic confining pressure for a range of saturations. Clear fundamental extensional resonance peaks and higher order harmonics are evident on each spectrum.

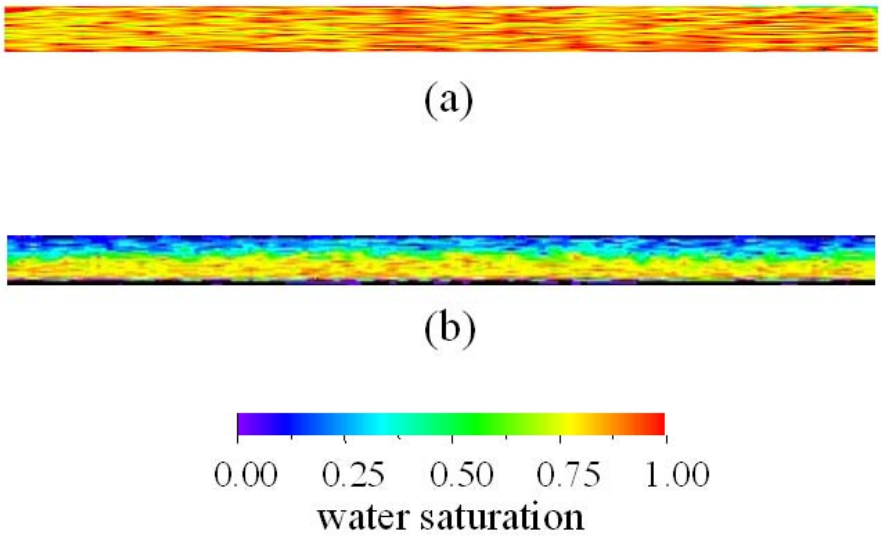

Figure 4. Water saturations obtained from X-ray CT scanning the sand samples: (a) *homogeneous* case with uniform distribution of water and gas (20 mm slices with 0.2 mm resolution; average water saturation is 90%), and (b) *horizontal-patchy* case with gas cap along the top (10 mm slices with 0.2 mm resolution; average water saturation is 60%). The length of the image is 81 cm, and the diameter is 43 mm.

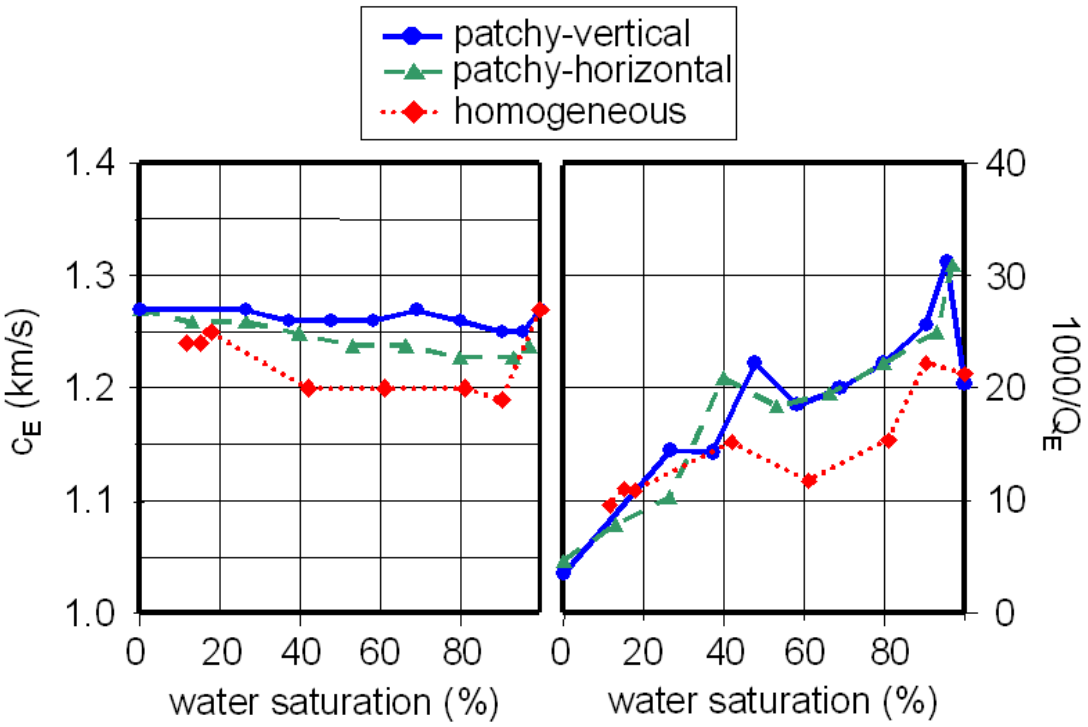

Figure 5. Extensional wave velocities and attenuation at 3 kHz for a range of water saturations and for three types of gas saturation: homogeneous, patchy-horizontal, and patchy-vertical.

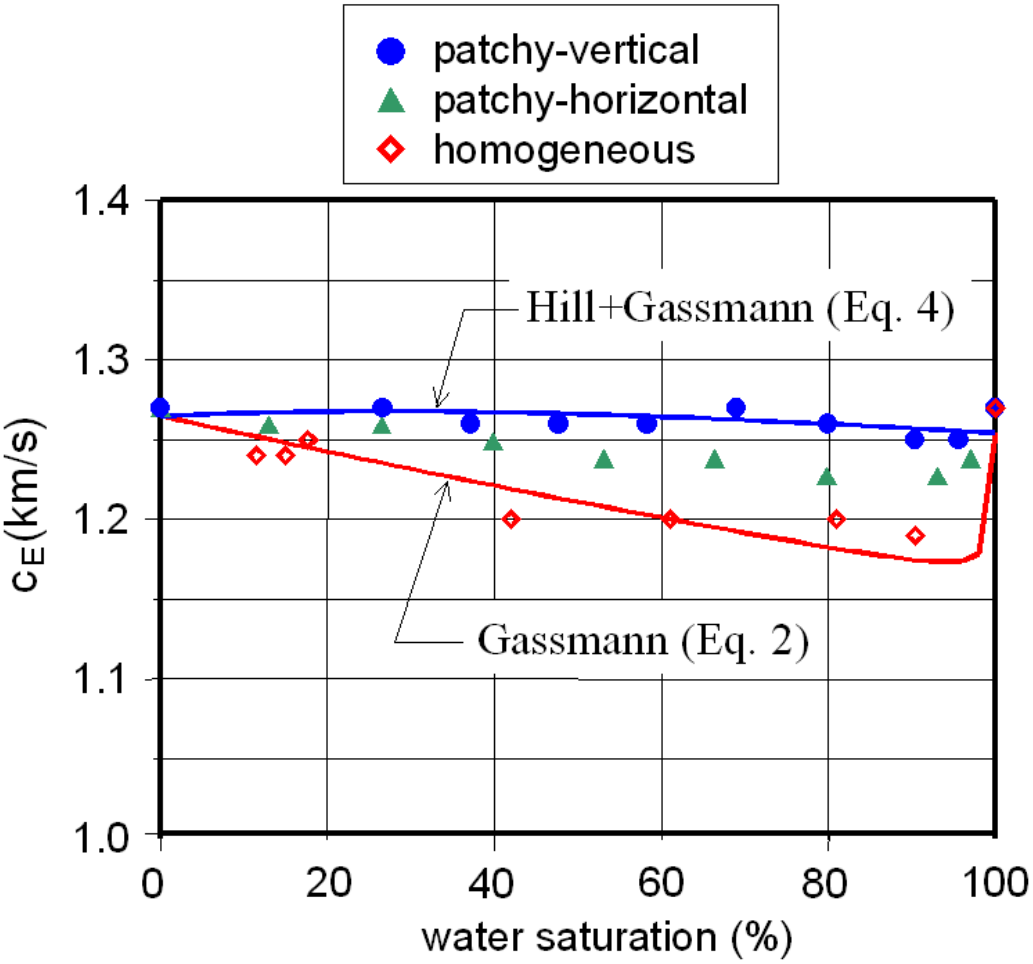

Figure 6. Comparison of measured extensional wave velocities with Gassmann theory (homogeneous case) and Hill+Gassmann (patchy-vertical case).